

# The catastrophic 1456 multiple earthquake: CFF test of interaction among deep oblique strike-slip faults in southern Italy

Umberto Fracassi\* and Bruna Perniola\*

\* Istituto Nazionale di Geofisica e Vulcanologia, Via di Vigna Murata 605, 00143 Roma, Italy (fracassi@ing.it)  
\* Istituto di Fisica, Università di Urbino, Via Santa Chiara 27, 61029 Urbino (PU), Italy

## Introduction: the 1456 multiple earthquake

In December 1456-January 1457 a major earthquake sequence took place across the central and southern Apennines (southern Italy, Calabrian Arc excluded), including southeastern Apulia (Magri and Molin, 1983; Meletti et al., 1988; Boschi et al., 2000). A recent re-evaluation of the (a) revised damage pattern and historical references for this multiple earthquake, (b) deeper seismicity of the southern Apennines – Adriatic foreland interface and (c) deep-seated regional E-W structures, led to the identification of at least four seismicogenic sources, responsible for the main sub-events of the multiple 1456 earthquake (Fracassi and Valensise, subm.).

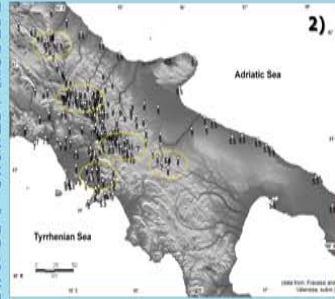
Based on various seismological, macroseismic and tectonic constraints, these causative faults are thought to exhibit an oblique right-lateral motion along fault segments roughly E-W oriented. Such segments are portions of well-known inherited regional E-W trending shear zones (like the Molise-Gondola shear zone), at various latitudes (between from north to south) the Maella Mt. and the Vulture volcanic complex. This system would therefore imply the cascade reactivation of such shear zones favorably oriented with respect to present stress field, with a transitional mechanism. More than one catastrophic historical earthquake that occurred in southern Italy suggests the nearly simultaneous activation of multiple sources across widely spaced ( $\pm 30$  km) portions of independent E-W faults. Being the strongest (by magnitude and damage area) among these major earthquakes, the 1456 sequence can be considered as a template for such mechanism of multiple activation of distant sources yet within a short time window.



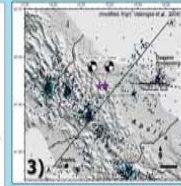
Historical ( $M > 4$ ) and main instrumental earthquakes

1) Black squares (proportional to magnitude) are events from Italy's current historical catalogues. Notice the predominance of (a) dip-slip re-activation of the NW-SE trending planes in the core of the thrustbelt and (b) strike-slip mechanisms in the eastern sector of the Apennines and in the Apulian foreland. Dark boxes indicate location of 1456 mainshocks in current catalogues (Gruppo di Lavoro CPTI, 2004).

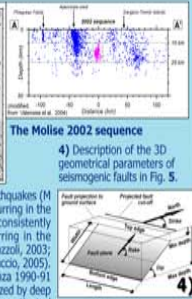
2) New macroseismic field of the 1456 sequence, showing the multiple areas of high damage (intensity  $> 8$ ) which, by distance and intensity distribution, are not compatible with the activation of a single major seismicogenic source.



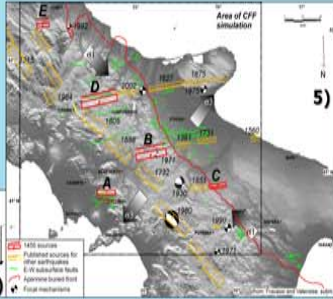
The revised intensity field of the 1456 earthquake



3) The 31 Oct-1 Nov 2002 Molise earthquakes (M 5.8) show that destructive events occurring in the Adriatic foreland have hypocenters consistently deeper ( $> 15$  km) than those occurring in the Apennines ( $< 15$  km) (Di Bucci and Mazzoli, 2003; Chiarabba et al., 2005; Valle and Di Luccio, 2005). The Molise earthquakes, like the Potenza 1990-91 ones (Di Luccio et al., 2005), characterized by deep ruptures on a E-W trending plane, reactivated segments of deep crustal E-W regional faults.



4) Description of the 3D geometrical parameters of seismicogenic faults in Fig. 5.



Our 5 seismicogenic sources to explain the 1456 earthquakes

ID	Strike (deg)	Dip (deg)	Rake (deg)	Length (km)	Width (km)	MinDepth (km)	MaxDepth (km)	Area (sq km)	Slip (cm)	$M_w$	$M_d$ (Nm)
A	275	70	220	17.8	11.0	11.0	21.2	194.0	0.65	6.3	4.61E+18
B	85	70	230	28.2	15.0	11.0	25.0	402.2	1.1	6.7	1.53E+19
C	268	80	180	17.5	11.0	11.0	21.8	192.5	0.65	6.3	4.13E+18
D	83	70	230	36.0	15.0	11.0	25.0	536.4	2.5	7.0	4.42E+19
E	89	70	230	12.0	8.0	11.0	18.5	96.0	0.45	6.0	1.43E+18

5) Proposed seismicogenic sources (in red) for the largest 1456 events. Large arrows show stress orientation after Montone et al. (2004). Notice that the hypothesized faults (particularly the largest ones, i.e. B and D) are constrained by the position and rake of the published seismicogenic sources (in orange) that caused the largest historical and instrumental earthquakes (years next to faults), NE-SW trending extensional faults are in the core of the Apennines, while E-W trending right-lateral strike-slip occurs towards the Apulian foreland (sources from: Valensise and Pantoli, 2001; DISS Working Group, 2005, and references thereon). Oblique slip  $\sim$  E-W oriented planes proposed for our sources would account for the transition from a purely extensional domain in the thrustbelt (i.e. the 1980 Itripina earthquake) to a strike-slip environment in the foreland (i.e. the 2002 Molise earthquake). This hypothesis considers the 1930 Itripina event (Palombo et al., 2004) as a template for such transition. Notice the  $\sim$  E-W structures known in the subsurface (shown in green, from: Sella et al., 1988; Bruno et al., 1998; Sawyer, 2001). All seismicogenic source parameters are summarized in upper inset; assigned chronology ranges from 5 Dec. (sources A, B and C, circa contemporaneous) to 30 Dec. (sources D and E, circa contemporaneous).

## The objective: to test fault interaction

After a thorough stratigraphic review (Guidoboni and Ferrari, 2004; Guidoboni and Comastri, 2005) on which Fracassi and Valensise (subm.) based the revision of the macroseismic pattern of the activation of the various sources that could explain such a damage pattern and catastrophic intensity distribution. Our attempt is to test (a) the possibility that the seismicogenic faults we devised can interact due to stress transfer, and (b) the relative chronology in the activation due to triggering among faults.

## The seismotectonic model

Our hypothesis invokes stress interaction between multiple sources falling within neighboring domains. We investigated Coulomb stress changes related to the main sub-events of the multiple 1456 earthquake to analyze fault interaction and stress transfer mechanisms. An evident positive correlation between the calculated Coulomb stress increase and three major seismicogenic sources is found. Therefore, the spatial redistribution and enhancement of static stress caused by the stronger events may promote rupture on adjacent faults that are close to the failure threshold. A more general case may be considered imposing a pre-existing stress field or assuming different values for the friction coefficient.

To the extents of present knowledge and investigation, these E-W trending earthquakes sources are active between ca. 10 and 20 km at depth in the sector of the southern Apennines east of the chain axis, that is to say in the seismicogenic macroregion bounded by the thrustbelt (to the west) and by the Apulian foreland (to the east). The stress patterns caused by these faults are consistent with the large NW-SE trending pure extensional sources found along the southern Apennines axis.

## The methodology

The method used to analyse stress transfer and fault interaction mechanisms is to compute the static stress due to the dislocation processes.

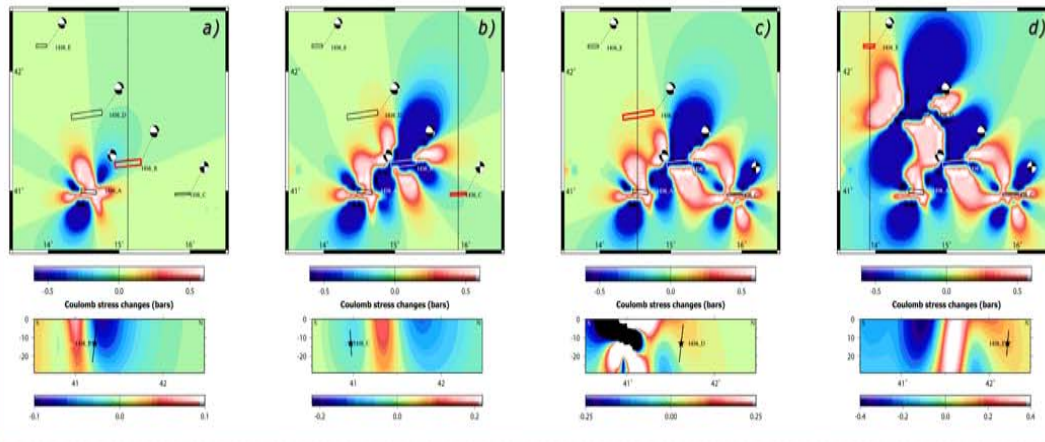
The coseismic stress changes caused by a dislocation on the master fault are expressed in shear and normal stress perturbations by projecting the computed stress tensor on a secondary fault.

The calculations are performed applying the Okada's equations for dislocations in an elastic homogeneous half-space (Okada, 1985; Nozoe et al., 1997). Moreover, Coulomb Failure Criterion is assumed to estimate the stress pattern (Harris and Simpson, 1992; Reasenberg and Simpson, 1992; Stein et al., 1994). The adopted equation for Coulomb Stress Changes takes into account the pore pressure as well. The availability of information about geometry and slip direction of the event rupture makes easy to calculate the changes of stress. If the geometry and faulting mechanism of receiver faults is known, it is possible to calculate the Coulomb stress changes due to an earthquake on the nearby faults.

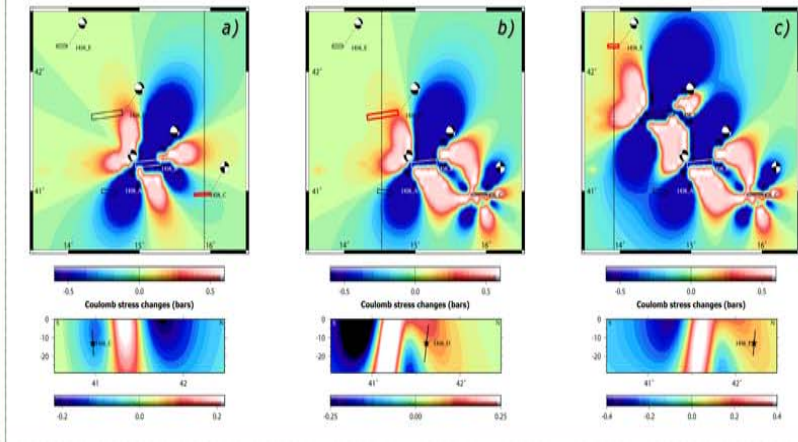
The approach can be different for aftershocks stress analyses, where the fault planes associated with these events are unknown. The solution is found searching the best planes for failure (optimally oriented 'fault planes'), where it is examined the Coulomb Stress (King et al., 1994). In the first section, we considered two models. They consist of 5 (M1 model) and 4 seismic sources (M2 model) respectively. The modeling presented shows the Coulomb Stress Changes calculated using the fault plane solutions and the rupture geometry obtained by M1 and M2 models.

The static stress changes are computed at Earth surface on a horizontal plane and on a vertical cross section oriented approximately north-south, perpendicular to the strike of the fault devised for each event (see dotted trace on each map). The source on which the interaction caused by stress transfer is projected is shown in thick red.

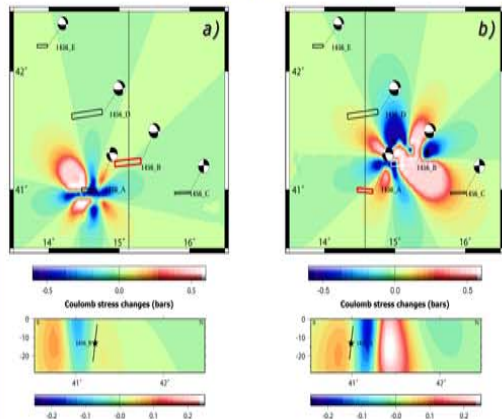
## Model M1



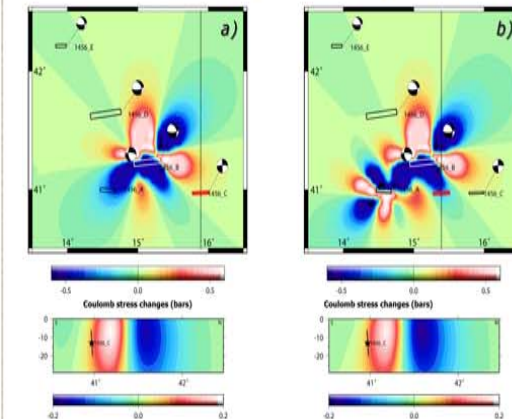
## Model M2



## Model R1 (sources AB)



## Model R2 (sources ABC)



## Model M1, 5 sources

(a) Coulomb stress changes caused by source A and calculated on fault plane B; (b) Coulomb stress changes caused by sources A and B and calculated on fault plane C; (c) Coulomb stress changes caused by sources A, B and C and calculated on fault plane D; (d) Coulomb stress changes caused by sources A, B, C and D and calculated on fault plane E.

## Model M2, 4 sources

(a) Coulomb stress changes caused by source B and calculated on fault plane C; (b) Coulomb stress changes caused by sources B and C and calculated on fault plane D; (c) Coulomb stress changes caused by sources B, C and D and calculated on fault plane E.

## Model R1 with regional input (sources A and B)

A pre-existing regional stress field with a nearly vertical compressive axis ( $\sigma_1$ ), an extensional stress axis sub-horizontal ( $\sigma_3$ ) oriented NE-SW, and a magnitude of 35 bars have been considered. (a) Coulomb stress changes caused by source A and calculated on fault plane B; (b) Coulomb stress changes caused by source B and calculated on fault plane A.

## Model R2 with regional input (sources A, B and C)

A pre-existing regional stress field with a nearly vertical compressive axis ( $\sigma_1$ ), an extensional stress axis sub-horizontal ( $\sigma_3$ ) oriented NE-SW, and a magnitude of 35 bars have been considered. (a) Coulomb stress changes caused by source B and calculated on fault plane C; (b) Coulomb stress changes caused by sources A and B and calculated on fault plane C.

## Results

The calculated stress pattern caused by the ruptures of previous events in both models (ABC for M1 and BC for M2) produced a Coulomb Stress increase in the area of sources D and E. Therefore, in both cases the results suggest that an elastic interaction exists among the major faults of 1456 earthquake.

As a last test, we investigated the possibility to invert the order of rupture of sources A e B. The positive Coulomb stress changes caused by source B in the A source area support this hypothesis.

## Conclusions

The hypothesis of multiple sources is confirmed by our experiments for both (a) source kinematics (oblique dextral slip on a  $\sim$  E-W trending fault plane and (b) chronology of the sequence. This result provides a valid support to (a) the fact that at least four large sources (and possibly five) are needed to explain the cumulative seismic moment release obtained with automatic methods from the revised intensity pattern and (b) the temporal sequence of the "casade" activation inferred from the historical constraints. Therefore, both the tectonic model is compatible with the stress transfer simulation and the reconstruction of the earthquake sequence.

While the CFF simulation does not support that source A could activate source B, the contrary could have happened if regional stress field is taken into account. However, historical sources to constrain the full chronology of the very first days of the sequence are not entirely clear, thus leaving room for speculation about the true order of activation between the two sources. Therefore, our simulation may provide with a physically more realistic interpretation of how the large source B and the comparatively smaller source A have interacted.

## References

Boschi, E., Guidoboni, E., Ferrari, G., Marotta, D., Valentini, G. and Gasperini, P., 2000. *Annali di Geofisica*, 43, 1-4.  
Boschi, E., Guidoboni, E., Ferrari, G., Marotta, D., Valentini, G., 2001. *Annali di Geofisica*, 44, 1-4.  
Chiarabba, C., Di Bucci, G., Molin, P. et al., 2005. *Annali di Geofisica*, 48, 1-4.  
Di Bucci, G., Chiarabba, C., Molin, P., 2003. *Annali di Geofisica*, 46, 1-4.  
Di Bucci, G., Chiarabba, C., Molin, P., 2004. *Annali di Geofisica*, 47, 1-4.  
Fracassi, U., Valensise, G., 2005. *Annali di Geofisica*, 48, 1-4.  
Gruppo di Lavoro CPTI, 2004. *Repertorio Nazionale degli Eventi Sismologici del CPTI 2004*.  
Harris, R. W. and Simpson, J. W., 1992. *Journal of Geophysical Research*, 97, 1205-1216.  
King, G. W., Stein, R. S. and Lin, J. C., 1994. *Journal of Geophysical Research*, 99, 1193-1204.  
Montone, I., 2004. *Annali di Geofisica*, 47, 1-4.  
Nozoe, H., 1997. *Journal of Geophysical Research*, 102, 1191-1201.  
Okada, Y., 1985. *Journal of Geophysical Research*, 90, 10911-10927.  
Palombo, G., 2004. *Annali di Geofisica*, 47, 1-4.  
Reasenberg, P. W. and Simpson, J. W., 1992. *Journal of Geophysical Research*, 97, 1205-1216.  
Sawyer, L. S., 2001. *Journal of Geophysical Research*, 106, 1193-1204.  
Sella, R. F., 1988. *Journal of Geophysical Research*, 93, 143-151.  
Stein, R. S., King, G. W. and Lin, J. C., 1994. *Journal of Geophysical Research*, 99, 1193-1204.  
Valensise, G., 2004. *Annali di Geofisica*, 47, 1-4.  
Valensise, G., Fracassi, U., and Bindi, P., 2004. *Annali di Geofisica*, 47, 1-4.